



Published in final edited form as:

Biochemistry. 2008 August 19; 47(33): 8804–8814. doi:10.1021/bi800297j.

Excluded volume effects upon protein stability in covalently crosslinked proteins with variable linker lengths[†]

Yun Ho Kim[‡] and Wesley E. Stites^{*}

Department of Chemistry and Biochemistry, University of Arkansas, Fayetteville AR 72701–1021, U.S.A.

Abstract

To explore the effects of molecular crowding and excluded volume upon protein stability a series of crosslinking reagents have been used with nine different single cysteine mutants of staphylococcal nuclease to make covalently linked dimers. These crosslinkers ranged in length from 10.5 Å to 21.3 Å, compelling separations which would normally be found only in the most concentrated protein solutions. The stabilities of the dimeric proteins and monomeric controls were determined by guanidine hydrochloride and thermal denaturation. Dimers with short linkers tend to show pronounced three state denaturation behavior, as opposed to the two state behavior of the monomeric controls. Increasing linker length leads to less pronounced three state behavior. The three state behavior is interpreted in a three state model where crosslinked native protein dimer, N-N, interconverts in a two state transition with a dimer where one protein subunit is denatured, N-D. The remaining native protein in turn can denature in another two state transition to a state, D-D, where both tethered proteins are denatured. Three state behavior is best explained by excluded volume effects in the denatured state. For many dimers, linkers longer than 17 Å removed most three state character. This sets a limit on the flexibility and size of the denatured state. Notably, in contradiction to theoretical predictions, these crosslinked dimers were not stabilized. The failure of these predictions is possibly due to neglect of the alteration in hydrophobic exposure that accompanies any significant reduction in the conformational space of the denatured state.

Keywords

denatured states; molecular crowding; excluded volume; main-chain entropy; conformational restriction

Levels of macromolecules are very high *in vivo* compared to the very dilute macromolecular concentrations commonly used *in vitro*.¹ This property of cells, often referred to as molecular crowding, has been recognized for some time (1,2) but more recently the question of how molecular crowding alters protein stability and association has attracted more widespread attention (3-9).

[†]This research was supported by NIH Grant NCRR COBRE 1 P20 RR15569.

^{*} To whom correspondence should be addressed. Tel: 479–575–7478, Fax : 479–575–4049. E-mail: wstites@uark.edu.

[‡]Present address: Department of Physical Sciences, Station 23, The University of West Alabama, Livingston, AL 35470–2099

Supporting Information Available

Details of the synthetic procedures for each crosslinker and their characterization are presented as are the details of crosslinking reaction yields and levels of free thiol measured by Ellman's assay. Thermodynamic parameters obtained from two and three state fits to data obtained from guanidine hydrochloride denaturation at 100 mM NaCl are also offered. This material is available free of charge via the Internet at <http://pubs.acs.org>.

Macromolecules are, of course, relatively large molecules. Inside a typical cell they occupy some 20–30% of space (5,10,11). The concentration of any one species is relatively low, hence the term “concentrated” is generally avoided in favor of “crowded,” but regardless of the terminology it is obvious that conditions are far from the condition of infinite dilution where a protein folds and unfolds in isolation.

Our interest here is addressing the impact of such conditions upon protein stability. Protein stability is free energy difference between the relatively compact and ordered native state and the disordered and relatively expanded denatured state. It is well accepted that the principal driving force for unfolding is entropy (12). The denatured state has much more conformational entropy than the native. In the absence of attractive or repulsive intramolecular interactions, excluded volume should conformationally limit the denatured state and hence destabilize it, thus increasing protein stability. The theory for this effect is well developed (10,13-18).

However, there is not a great deal of experimental evidence on this issue. Monitoring the effect upon one particular relatively dilute protein species in a complex soup of other proteins present in large amounts presents obvious experimental difficulties. Eggers and Valentine (19) used another method to avoid this problem, mimicking the effects of confinement and crowding on the structure and stability of proteins by enclosing the proteins within the pores of sol-gel glass. They found that this increased the melting temperature of α -lactalbumin by as much as 32 °C. On the other hand, other proteins did not show any increase in stability. Similarly, Flaugh and Lumb (20) tested the hypothesis that the intrinsically disordered proteins c-Fos and p27^{Kip1} would adopt folded structures under crowded conditions in which excluded volume is predicted to stabilize compact, native conformations. Using dextrans and Ficoll to provide molecular crowding effects, they found no induced ordered structure in these normally disordered proteins. Similarly, the stability of FK-506-binding protein was found to be minimally affected by Ficoll (21).

Aside from the sparse number of studies addressing this issue, there is an important question about such work. The physiological relevance of dextran, Ficoll, and, especially, silica glass is unclear. Further, the size and shape of the pores in a glass is to some degree heterogenous and uncertain.

Previous work by our research group has been aimed at addressing precisely this issue of excluded volume. We used the strategy of introducing intramolecular cross-links in the model protein, staphylococcal nuclease, using the cysteine specific cross-linking reagent 1,6-bismaleimido-hexane (BMH) (22). There are no cysteines in wild-type staphylococcal nuclease, so single cysteine substitutions were engineered onto the protein surface providing specific sites for alkylation with crosslinking reagent. After crosslinking, the covalent dimers were purified. Covalent linkage restrains the two proteins at a comparatively well defined distance and orientation.

Guanidine hydrochloride (GuHCl) denaturation of the crossed-linked dimers showed biphasic unfolding behavior that did not fit the two state model of unfolding. These crosslinked dimers were fitted to a three state thermodynamic model (both monomer subunits in the native (N-N), one monomer subunit native and one denatured (N-D), and both monomer subunits denatured (D-D)) of two unfolding transitions in which the individual subunits cooperatively unfold. These two unfolding transitions were very different from the unfolding of the monomeric protein.

These differences in unfolding behavior were attributed in large part to changes in the denatured state, changes which are thought to be due to the exclusion of nearby volume by the other half of the dimer. If this interpretation is correct it is direct evidence that excluded volume effects in crowded protein solutions are significant. However, it is important to note that, in contrast

to theoretical predictions, we did not observe increases in protein stability. Indeed, the stability of the dimers was usually significantly lowered relative to monomers. Some of this appears to be native state effects, but we argued that reducing the volume accessible to the denatured state also reduced hydrophobic exposure and hence stabilized the denatured state, an effect neglected in theoretical treatments.

The crosslinked dimers were also thermally unfolded. In contrast to the GuHCl denaturations, thermal denaturation fitted to a two state model well, but with greatly elevated van't Hoff enthalpies in many cases. These changes in thermal denaturation that fit a two state model can be rationalized by hydrophobic interactions in the denatured states as well.

This previous work used only one length of crosslinker. We felt an obvious and useful extension would be to see how the effects of crosslinking varied with linker length. Accordingly, in this study we have synthesized four different length bis-maleimide crosslinkers, related to the BMH used in our first study, and three different length haloacetamide crosslinkers. Using the same nine cysteine mutants of staphylococcal nuclease as before (G29C, G50C, E57C, A60C, K70C, K78C, R105C, A112C, and K134C) we have found very clear and interesting trends as the length of the tether linking the two protein molecules increases.

Experimental Procedures

Protein expression and purification

Wild type and all nine single cysteine mutants of the model protein, staphylococcal nuclease, were prepared as previously described (22,23).

Synthesis of crosslinkers

Details of the synthesis of the crosslinkers is available as supporting information. The identity of all crosslinkers was verified by ^1H NMR (Bruker, 300 MHz) and purity was confirmed by analytical reverse phase HPLC using a Waters 600E system with 991 photodiode array detector. Single peaks, monitored at 215 nm, free of precursors, were found for all crosslinkers.

Crosslinking reaction

Each linker was dissolved in DMSO to make a 15mM stock solution. Nine different cysteine single mutants, substituted at glycines 29 or 50 (G29C, G50C), glutamate 57 (E57C), alanines 60 or 112 (A60C, A112C), lysines 70, 78, or 134 (K70C, K78C, K134C), and arginine 105 (R105C) were used, as well as a wild-type control. Wild-type staphylococcal nuclease has no cysteines and a molecular weight of 16,843 daltons. All proteins were employed in the crosslinking reaction at 10.5 mg/mL (623 μM) concentration.

Typically, ten mg (952 μL , 593 nmol) of purified cysteine mutant or wild type was treated with 1 equivalent of bismaleimides (**1**–**4**) or bishaloacetamide (**5**–**12**) in 25 mM sodium phosphate, 100 mM NaCl at pH 7.0. Each crosslinker (19.8 μL , 297 nmol) was added (1:2 crosslinker to protein mole ratio) as a 15 mM solution in DMSO. The reactions were carried out in 4 dram borosilicate vials at room temperature for 6 hours while being agitated with “flea” stir bars. To the reaction mixture, 3 volumes of cold ethanol were added and incubated at -20°C for 30 minutes. The precipitate was then spun at 14K rpm in a refrigerated microcentrifuge for 10 minutes at 4°C . After discarding the supernate, the resulting pellet was resuspended in 1 ml of denaturing and reducing buffer (25 mM sodium phosphate, 100 mM NaCl, 2 M guanidine hydrochloride, 10 mM β -mercaptoethanol (2-thioethanol, BME), pH 7.0).

Separation of Protein Dimers and Monomers

The crude protein was purified using a Water 600e HPLC equipped with Pharmacia Superdex 16/60 gel filtration column using a denaturing and reducing buffer (25mM sodium phosphate, 100mM NaCl, 2M guanidine hydrochloride, 10mM BME, pH 7.0) while being monitored with a photodiode array detector. Integration was performed at 280 nm. Complete baseline resolution was not achieved, although it was sufficient for peak integration and determination of relative yields of dimer. Collected dimer fractions, cut conservatively from the front of the peak, were combined, concentrated using a Centricon filter unit to approximately 2 mg/ml, and repurified under the same conditions. The final repurified dimer fractions were combined, concentrated using a Centricon filter unit to approximately 1 mg/ml, and dialyzed twice against 25 mM sodium phosphate, 100 mM NaCl, pH 7.0. Injection of analytical amounts confirmed the absence of monomeric protein.

Ellman's Assay

All purified crosslinked dimers using bismaleimide (n=0 to 3) and haloacetamide (n=0 to 2) crosslinkers and modified monomeric controls made using N-(2-hydroxyethyl)maleimide (HEM) and 2-bromo-N-(2-hydroxyethyl)-acetamide (BHA) were subjected to a standard Ellman's assay (24) to quantify the extent of reaction at cysteine residues. Wild-type and unreacted cysteine mutants were also assayed as controls.

Solvent denaturations

In general, guanidine hydrochloride (GuHCl) denaturation, followed by fluorescence, were carried out as described elsewhere (25,26). Tricarboxyethyl phosphine (TCEP, 0.5 mM) was added to proteins with free thiols to prevent disulfide formation. In one change from our usual procedure, the denaturations were carried out at both the usual 100 and at 250 mM sodium chloride. Data analysis using a two state model was carried out as previously described (25). The denaturation data for all crosslinked dimers were also analyzed by a three state thermodynamic unfolding model previously described (22).

Thermal denaturations

Thermal denaturations, followed by fluorescence, and data analysis were performed as previously described (22).

Molecular modeling

In order to estimate the maximum sulfur to sulfur distance of each crosslinker, the Hyperchem 7 Molecular Modeling program (Hypercube Inc.) was used to optimize each crosslinker, modified with methyl thiol, in an extended conformation. Various stereochemistries and orientations of the two sulfur modified reactive groups were modeled to determine which gave the maximal separation.

Results

Crosslinking

Detailed results of the yields of each crosslinking reaction and of the Ellman's assay confirming that the crosslinking reaction blocked all free cysteines, leading to a dimeric product with defined points of covalent attachment, are available in supporting information.

Guanidine hydrochloride denaturations

The stability to reversible solvent denaturation of all purified dimers, unreacted monomers, and monomers reacted with monofunctional controls was characterized by fluorescence

spectroscopy. Nuclease possesses a single tryptophan located at position 140 which can act as a sensitive probe of structure to distinguish whether the protein molecule is folded or unfolded. Normally the staphylococcal nuclease and its mutants have very well behaved denaturations, with a clear sigmoidal curve with relatively flat native and denatured baselines. We noted a tendency for the dimeric proteins to have native baselines with pronounced curvature, which greatly complicates data analysis. For reasons that are not clear to us, such behavior was not as noticeable in our previous BMH crosslinking work. The possibility that this was due to electrostatic interactions in the native state was considered and therefore denaturations of the bis-maleimide crosslinked dimers were also carried out at a higher ionic strength than normal (250 mM versus 100 mM NaCl). At higher ionic strength the baseline curvature was significantly reduced on all cases. The titrations of the haloacetamide crosslinked dimers were only carried out at 250 mM NaCl. The titration behavior of representative crosslinked dimers at both ionic strengths is shown in Figure 1.

Analysis of guanidine hydrochloride (GuHCl) denaturations in terms of a simple two state model yields three parameters: a protein's stability to reversible denaturation in the absence of denaturant (ΔG_{H_2O}), the rate of change of free energy with respect to GuHCl concentration (m_{GuHCl} or $d(\Delta G)/d[GuHCl]$), and the concentration of guanidine hydrochloride at which half the protein molecules are denatured (C_m). These parameters are shown in Table 1 for the unmodified cysteine mutants and wild-type, and for these same proteins after treatment with the monovalent controls HEM and BHA.

The average change in free energy for the control (HEM) modified monomers relative to unmodified protein ($\Delta G_{cysteine\ standard} - \Delta G_{HEM\ monomer}$) is only 0.1 ± 0.1 kcal/mol, in other words, unchanged within experimental error. While around 25% of the HEM treated proteins are unmodified, based on Ellman's assay, this small change in stability still seems to indicate that derivatization of cysteine with maleimide does not by itself cause significant stability changes. The stability changes for wild-type are somewhat higher, perhaps since the absence of cysteines means reactions with other side chains, with more deleterious effects, are more likely.

In line with this idea, when enough monomer could be recovered for stability measurements after treatment with bismaleimide rather larger changes in stability are found (data not shown). The average change in free energy for the bismaleimide treated monomers is 1.2 ± 0.1 kcal/mol. This likely reflects the fact that while reaction with cysteine is preferred, it is not the only possible course of reaction. Many of these monomers have probably been intramolecularly crosslinked.

Many of the crosslinked dimers exhibit clear biphasic unfolding behavior, as most clearly shown in Figure 1 for the dimer of K78C. Therefore, the three state model describing the thermodynamics of unfolding for these dimers as outlined in materials and methods was fit to data for these proteins. Our model assumes at any given guanidine hydrochloride concentration only three species are significantly populated. Those species are described as follows: crosslinked dimer with both monomer units folded (N-N), crosslinked dimer with one monomer unit folded and one unfolded (N-D), and crosslinked dimer with both monomer units unfolded (D-D). Also, we assume that each phase of the denaturation can be described by a single cooperative transition and in fitting we assume that one-half of fluorescence difference between the N-N state and D-D state is lost in the N-D state. Each phase can be characterized by a unique slope value and free energy. These values are given in Table 2 for dimers attached with the bismaleimide crosslinker family and in Table 3 for selected dimers resulting from crosslinking with the bis-haloacetamide family. The results of three state fits to the denaturations of the bismaleimide dimers at 100 mM NaCl are available in the supporting information. Other models of unfolding are theoretically possible, for example, both monomers

might simultaneously partially unfold and then later completely unfold cooperatively (N-N to I-I to D-D). This can not be completely ruled out, but it seems unlikely because it is widely thought that the first structure to unfold in nuclease is the C-terminal helix containing the tryptophan and postulating a partially unfolded intermediate that retains tryptophan fluorescence would be without precedent.

Particularly for long linker lengths, the transitions of some proteins no longer exhibit clear three state behavior. All of the data were also analyzed with a two state model and those results are given in Table 4 for dimers attached with the bis-maleimide crosslinked dimers and in Table 5 for selected dimers resulting from crosslinking with the bis-haloacetamide family. The results of two state fits to the denaturations of the bis-maleimide dimers at 100 mM NaCl are available in the supporting information. The fit of the data to the linear two state model is given as well to aid in evaluation of the reliability of this model. Normally, for monomeric mutants we consider a value of R^2 of less than 0.999 an indication of poor data quality.

Lastly, a description of the error associated with the non-linear regressions to the three state model is needed. The average errors returned by the fitting program for ΔG_{H_2O} of the first (N-N \rightleftharpoons N-D) transition were ± 0.2 kcal/mol and for the second (N-D \rightleftharpoons D-D) transition were ± 0.5 kcal/mol. For both transitions the errors in m_{GuHCl} were close to ± 0.5 kcal/(mol·M). However, these average numbers hide a large range. The lowest reported uncertainties for m_{GuHCl} were ± 0.07 kcal/(mol·M) and the highest were ± 1.8 kcal/(mol·M). The lowest reported uncertainties for ΔG_{H_2O} were ± 0.03 kcal/mol and the highest were ± 1.8 kcal/mol. Uncertainty in one parameter was well correlated with uncertainty in others. Specifically, when uncertainty in the parameters for the slope was high, so was uncertainty in the stability. Uncertainty in the first transition also correlated extremely well to uncertainty in the parameters for the second transition.

The error reported by the fitting program was generally lowest when there were two distinct transitions, *i.e.* when a three state unfolding was clearly present and the data constrained the possible range of solutions. Errors were higher when there were not two distinct transitions visible. In this case, the available data undetermined the fitting of the complex equation for the three state model and a fairly wide range of possible solutions exists. Nevertheless, it should be noted that similar parameters for the two transitions were still returned when fitting these cases, despite their higher uncertainty. The major exception to this trend was R105C, which has two transitions, but had high uncertainties. This is presumably due to the fact that it is partially unfolded even in the absence of denaturant and no native baseline exists to constrain the fits. The values for m_{GuHCl} in the first transition, especially for the shortest linkers, are suspiciously high and it seems likely that the relatively large error returned by the fitting program for the various R105C dimers is, if anything, too low. In summary, except for R105C, when there are large differences between m_{GuHCl} or ΔG_{H_2O} for the two transitions in Table 2 or 3, the confidence in these values is high. When differences are relatively small, uncertainties are high and the actual difference might possibly be larger, or completely negligible.

Thermal denaturations

The thermal unfolding of the crosslinked dimers was followed by fluorescence spectroscopy, except for the dimers of the R105C mutant, which is too unstable to obtain reliable native baseline data needed for the data analysis. As previously found for the BMH crosslinked dimers, even in 100 mM NaCl, the data was well fit in all cases by a standard two state model. The results of this analysis are shown in Tables 6 where T_m is that temperature at which half of the protein molecules are unfolded and ΔH_{vH} is the van't Hoff enthalpy of unfolding at the transition temperature.

Discussion

Protein denatured states have been reviewed several times recently (27-30). Arguably, the denatured state of staphylococcal nuclease (nuclease) has been more intensively studied and is better understood than for any other protein. Unfortunately, the results of the study of nuclease are in many ways contradictory and confusing and thus illustrate how much remains to be learned about denatured states.

Still, we know that nuclease has, as do virtually all proteins examined, significant amounts of residual structure in the denatured state. The “structure” of denatured nuclease has been solved by NMR techniques by Shortle's group (31-34). They demonstrated that nuclease retains long range structure similar to the native state even under the highly denaturing conditions of 8 M urea. However, we know little about the relative flexibility of the different parts of the molecule. A particular question of interest is how far out the energetic “sphere of influence” of a denatured protein extends. In other words, how much space is required for the denatured protein to behave as if it is, in effect, isolated from other protein molecules?

As described in supporting information, we synthesized series of homobifunctional crosslinkers with differing lengths, based on a polyethylene glycol linker. These crosslinkers are shown in Figure 2. The sulfur to sulfur separation expected for each crosslinker at maximal extension is shown in Table 7. Three different thiol-specific functional groups were used: maleimide, bromoacetamide, and iodoacetamide. Previous work with a single length of crosslinker (22) established the specificity and completeness of modification with maleimide crosslinker and that the impact of alkylation itself upon protein stability was not extraordinary. Results presented in the supporting information, including those with a new control which is more polar than our previous control, reaffirm that earlier conclusion. The changes in protein denaturation behavior observed are therefore due to the constrained presence of another protein molecule, not to some other effect of the modification.

The alkylation of cysteine with bromoacetamide and iodoacetamide results in identical products, but the two groups differ in their specificity of reaction with thiol. The haloacetamides result in a quite different adduct from the maleimide. All proteins were reacted with the complete range of bis-maleimide crosslinkers. A selection of proteins reacted with bis-haloacetamide crosslinkers were also examined. These serve as yet another set of controls, confirming that similar behavior is found with crosslinkers of similar length, despite differences in the precise chemical group used to covalently link the proteins.

One effect that was observed, particularly prominently for short crosslinker lengths, was a tendency for the native baseline to rise with the addition of guanidine hydrochloride. It seemed likely that this effect was due to electrostatic interactions between the linked native states that are masked as the addition of guanidine hydrochloride raises ionic strength. Running the titrations in a buffer containing 250 mM NaCl rather than our normal 100 mM NaCl resulted in flatter baselines. A further advantage is that attenuating charge-charge interactions in both the native and denatured states should emphasize the influence of steric effects in the denatured state, something of particular interest. While this discussion will focus on the data obtained for dimers and the controls at 250 mM NaCl the results at lower ionic strength are available as supporting information.

It should be noted that such an increase in sodium chloride concentration has no significant effect upon the denaturation behavior of (monomeric) wild-type. We will return to this point later, but briefly, several dimers show distinct shifts in the midpoint of denaturation to lower concentrations of guanidine hydrochloride with higher concentrations of sodium chloride, while others show virtually no change other than a flatter native baseline.

Solvent Denaturation of Crosslinked Dimers

As expected, the guanidine hydrochloride denaturations of the unmodified standards and the HEM modified monomers fit the two state model of denaturation well, unfolding cooperatively in one transition. As inspection of Figure 1 shows, this is not true for many of the maleimide crosslinked dimers. In particular K78C and R105C show obvious deviations from the sigmoid behavior of the two state model. Although more subtle when looking at the raw denaturation curves, K70C, A112C, and K134C for some linker lengths do not have the strictly linear relationship between guanidine hydrochloride concentration and free energy predicted by the two state model (data not shown). On the other hand, many of the dimers, especially at longer linker lengths do seem to have two state denaturation curves.

This qualitative assessment is conveyed in a slightly more quantitative manner by comparing the protein stabilities determined by fitting to the two state model for the HEM alkylated controls and the dimers made using the various length crosslinkers. These differences, shown in Table 8, are striking. For some proteins, for example, G29C in Figure 1, there is never any experimentally significant difference between the monomeric control and the dimeric protein, regardless of linker length. For other proteins, for example, K78C, the dimeric protein is always significantly different from the monomeric control. For other proteins, for example, K70C, there are small differences at the shortest linker lengths that become experimentally insignificant as lengths increase.

It is important to recognize that a large *apparent* stability difference is not a valid measure of change in stability. Rather, what it does indicate is a case where the two state model has failed. Where the fit to the two state model is good for the dimer, there is little or no significant stability difference between dimer and monomeric control. Where the fit is poor, which in most cases corresponds to those protein dimers where there is clear cut biphasic unfolding, there is an apparent energy difference.

This biphasic unfolding behavior observed for some bismaleimide crosslinked dimers can be accounted for by postulating a three state thermodynamic model for the denaturation. These three states are a crosslinked dimer with both monomer subunits folded (N-N), a crosslinked dimer with one monomer subunit folded and one unfolded (N-D), and crosslinked dimer with both monomer subunits unfolded (D-D). We assume that each of the monomer subunits in the maleimide crosslinked dimers are independent folding units. The first transition follows the unfolding of one of the monomer subunits while the second transition follows the unfolding of the second monomer subunit. It is expected that these transitions are different. The first subunit unfolds while it is covalently bonded to another folded subunit and the second subunit unfolds while it is bonded to an unfolded subunit. These are distinctly different denaturations and hence each should be characterized by a unique free energy and slope value. The derivation of our three state unfolding mathematical model has been described previously (22). When non-linear regression is used to fit the data to the three state model, distinctly different m_{GuHCl} and $\Delta G_{\text{H}_2\text{O}}$ values are often found for the two transitions, as shown in Tables 2 and 3. Each of these transitions differs to a lesser or greater extent from those found for the modified monomers we use as controls (Table 1).

Comparison of Table 2 to Table 4 and of Table 3 to Table 5 shows that if the two state fit is good for the dimer then the three state fit generally, although not always, yields values for the component transitions that are very similar to one another and to the values from the two state fit. That there is disagreement between the three sets of values is not unexpected given the relative complexity of the three state model and the lack of two clearly resolved transitions in the data which the two state model fits. In other words, in many cases there is no significant difference between the results of the three state fit and the two state fit. There are obvious variations with linker length and position of crosslinker attachment that we shall return to.

More interesting are those dimers for which there are two distinct transitions. This would include K78C, R105C, and A112C dimers with all linker lengths and K70C, K134C, and, to a lesser extent, E57C dimers with shorter linker lengths. Here the differences between the two transitions returned by fitting to the three state model are much more meaningful. Some trends are found among cases where the three state model is clearly more appropriate. Previously, when we examined the effect of only a single linker length (22) it appeared that the stability, $\Delta G_{H_2O}^2$, of the transition between the N-D and D-D states was usually less than the stability determined for the first transition ($\Delta G_{H_2O}^1$), that between the N-N and N-D states. That generalization is still true, but now we find more exceptions, especially for long linkers.

We see that there is more variation in the values of stability, slope, and midpoint for the second transition as a function of linker length than for the first transition. While this variation does not seem to be a simple linear progression with increasing linker length, there is an overall tendency for the values of the first and second transition to converge with increasing length. In other words, the denaturation begins to look like a two state transition.

Previously (22) we had drawn the conclusion that the similarity of the first transition to that of monomeric controls and the generally reduced slope values for the second transition pointed to interactions between the denatured states as the cause of altered behavior for the second transition. Although it does not prove that changes in the denatured state are at the heart of this three state behavior, this tendency for the two transitions to converge with increasing length of the linker is consistent with that interpretation.

Thermal Denaturation of Crosslinked Dimers

Thermal denaturations of the bis-maleimide crosslinked dimers, HEM modified monomers and the unmodified cysteine standards were performed using fluorescence as a probe of structure. The temperature required to half unfold the protein (midpoint temperature, T_m) and the van't Hoff enthalpy (ΔH_{vH}) of unfolding at the T_m were obtained from the analysis of thermal denaturation data.

These results are shown in Table 6. T_m is down slightly for all the bismaleimide dimers relative to HEM modified monomers, but virtually invariant as a function of linker length. The van't Hoff enthalpies for eight of the bismaleimide crosslinked dimers are significantly higher than the untreated cysteine standards. The T_m is, within experimental error, virtually invariant as crosslinker length varies for a given mutant. However the van't Hoff enthalpy tends to drop slightly. As observed previously, the thermal unfolding data of the dimers does not reveal three state thermodynamic behavior but does generally show elevated van't Hoff enthalpies for the dimers relative to the HEM modified monomers. However, the dimers which fit the two state solvent denaturation model well, for example G29C, have van't Hoff enthalpies very similar to the HEM modified monomers. The more pronounced the three state behavior in solvent denaturation, the greater the elevation of ΔH_{vH} in thermal denaturation. Yet, even in these cases, the value of ΔH_{vH} tends to drop toward the value found in the HEM modified monomer as the linker length increases. Thus, there is obvious and consistent agreement between the thermal and chemical denaturation behavior for different sites of crosslinking and for different crosslinker lengths.

Positional Variation

There is clear variation in behavior with the position of alkylation. The sites chosen for derivatization are all solvent exposed in wild-type, but are scattered about the surface to provide a global sampling of behavior. Some positions have virtually no difference in either solvent or thermal denaturation behavior between alkylated monomeric control and the dimers. The most

clear case of this sort is G29C. G50C, E57C, and A60C show less clear cut two state behavior for the shorter linkers, but denaturation of the dimers is generally fairly similar to the monomers. K70C and K134C clearly are three state for the shortest linkers but are two state as the linker lengthens. A112C has a three state solvent denaturation for all lengths although the thermal denaturation of the longest linker seems to be fairly similar to the monomer. K78C and R105C are unambiguously different from the corresponding monomeric controls for all linker lengths in both solvent and thermal denaturation.

When these positions are plotted on the protein structure a clear pattern is obvious. The positions with the most pronounced three state behavior, K78C, R105C, and A112C, although well separated in primary structure, are all close to the C-terminal helix of nuclease (Figure 3). K70C is further away, but not as far as G29C, G50C, E57C, and A60C. K134C is at the very end of the C-terminal helix.

There are several indications that the C-terminus of nuclease is among the first parts of the protein to lose all structure. Most notable is the more rapid loss of fluorescence from tryptophan 140, than for a tryptophan added into the major hydrophobic core in the V66W mutant (35-38). This helix may or may not be a separate domain, however, there is no question that it is not an integral part of the beta barrel which makes up the largest part of the protein, and may unfold first (39-41). It is plausible that it is more disordered and enjoys greater conformational freedom in the denatured state than the rest of the protein, which is known to, overall, retain an expanded native-like structure (31,33).

Conformational Entropy and Protein Stability

The principal force of destabilizing the structure of protein is believed to be the high conformational entropy of the denatured state. Obviously the flexible denatured state has a much greater conformational freedom than the native state of a protein. It has been convincingly argued that this conformational freedom and, thus, the entropy of the protein's denatured state is limited by the volume occupied by the protein itself (42). It is expected that minimizing the conformational degrees of freedom in the denatured state would lead to destabilization of the denatured state and hence stabilization of the native state. However, the volume effect also can be a possible reason for increases in stabilities sometimes observed when proteins are linked to solid supports (43-46).

The denatured state of a protein is not a single discrete, well defined conformation but an ensemble of conformations. Consider for a moment the possibilities of restraining the conformational freedom of the denatured protein by crosslinking a protein to some object, which could be a macroscopic surface or another protein, either native or denatured. In Figure 4 a particular hypothetical denatured state conformation linked to such an object is illustrated schematically. In this conformation suppose that attachment point A is on the surface or near to it. A linker of modest length allows attachment to another object. However, another potential attachment point, B, is not near the surface of this conformation of the denatured state. Attachment at point B to another object with a short linker is not possible. Of course, the conformationally flexible denatured state can adopt another conformation, but the conformation illustrated in the figure and any others which significantly sequester the attachment from ready access are barred to it. In other words, the conformational freedom of the denatured state, the principal property favoring it relative to the native state, is reduced.

Again, the attachment points chosen are all solvent exposed in the native state, but since the residual structure in the denatured state is known to be native like, it seems plausible that these sites are usually solvent exposed in the denatured state. Given the minimal impact for the effect of crosslinking at, for example, G29C, it seems that this position is never inaccessible, even with our shortest crosslinker. On the other hand, even though they are solvent exposed, it is

easy to imagine looking at Figure 4 that another protein tethered at any of these points could significantly restrict the conformational freedom of the C-terminus if the helix detaches from the remainder of the structure, as we hypothesize that it does.

In short, the data presented here indicate clearly that excluded volume effects are real and readily observable. However, they also indicate that for most regions of this protein, that the denatured state is not so conformationally flexible that surface positions in the native state become deeply buried in the denatured state. There are some effects for the shortest linker length (circa 10 Å) but to place that in context, such a linker puts an entire other protein molecule at about the distance of the amine group on a lysine side chain.

There is another interesting observation in this data, which confirms our previous work with a single linker length. There is a presumption in the literature on excluded volume and molecular crowding that these effects will act to stabilize the native states of proteins. As we previously pointed out, this is not necessarily the case. In the data here where an excluded volume effect is clearly present the native state is *less* stable relative to the denature state, not more. Although native state effects cannot be ruled out, we speculated earlier (22) that this may be due the fact that a more compact denatured state fails to expose as much hydrophobic surface and this burial, in effect, counteracts some of the expected stability gains from lost conformational entropy. We find no reason in the data presented here to alter that view. It may be that restriction to compact denatured states does not require a large loss of conformational entropy (42). If this is true, and there is a little difference in the hydrophobic surface exposed in native state and in the restricted denatured state, our results are simply explained.

Lastly, the convergence of dimer denaturation behavior with that of monomers as linker length increases gives an interesting calibration for expected effects of molecular crowding. Most effects are lost or sharply attenuated by the time we reach a linker length of approximately 21 Å for $n = 3$. Admittedly, this is an attachment at only at one point on the protein surface and the protein is not crowded on all sides, but it does suggest that an average separation between molecules of more than 20 Å should suffice to remove most excluded volume effects. The radius of gyration of thermally denatured nuclease has been reported as 42 Å (47). When measured by small angle x-ray scattering, both the guanidine hydrochloride denatured wild-type protein and an unstable mutant in guanidine hydrochloride have similar radii of gyration, 37.2 ± 1.2 Å (48) and 38.8 Å (49) respectively. Even more compact than these values is the 33 ± 1 Å radius of gyration of wild-type in 8 M urea (50). Taking the first value as worst case and adding half of the linker length where effects disappear implies that each protein needs a sphere, on average, of no more than 53 Å to avoid excluded volume effects. This corresponds to the situation expected at a nuclease concentration of about 1.7 mM or 28 mg/ml. This is a fairly high concentration, but not incredibly so. This rough calculation extrapolating from results on one protein should not be taken too seriously, but it does imply that molecular crowding effects upon protein stability should indeed be observed at high protein concentrations, such as those found in the cell. However, the assumption that these effects will act to stabilize the native states of proteins relative to the denatured states should be carefully re-examined.

Supplementary Material

Refer to Web version on PubMed Central for supplementary material.

Abbreviations

BMH, 1,6-bismaleimido-hexane; GuHCl, guanidine hydrochloride; BME, β -mercaptoethanol; HEM, N-(2-hydroxyethyl)maleimide; BHA, 2-bromo-N-(2-hydroxyethyl)-acetamide; TCEP, tricarboxyethyl phosphine.

References

1. Zimmerman SB, Minton AP. Macromolecular crowding: biochemical, biophysical, and physiological consequences. *Annu Rev Biophys Biomol Struct* 1993;22:27–65. [PubMed: 7688609]
2. Minton AP. Confinement as a determinant of macromolecular structure and reactivity. *Biophys J* 1992;63:1090–1100. [PubMed: 1420928]
3. Minton AP. Influence of excluded volume upon macromolecular structure and associations in ‘crowded’ media. *Curr Opin Biotechnol* 1997;8:65–69. [PubMed: 9013656]
4. Ping G, Yuan JM, Sun Z, Wei Y. Studies of effects of macromolecular crowding and confinement on protein folding and protein stability. *J Mol Recognit* 2004;17:433–440. [PubMed: 15362102]
5. Ellis RJ. Macromolecular crowding: obvious but underappreciated. *Trends Biochem Sci* 2001;26:597–604. [PubMed: 11590012]
6. Chebotareva NA, Kurganov BI, Livanova NB. Biochemical effects of molecular crowding. *Biochemistry (Mosc)* 2004;69:1239–1251. [PubMed: 15627378]
7. Hall D, Minton AP. Macromolecular crowding: qualitative and semiquantitative successes, quantitative challenges. *Biochim Biophys Acta* 2003;1649:127–139. [PubMed: 12878031]
8. Despa F, Orgill DP, Lee RC. Molecular crowding effects on protein stability. *Annals of the New York Academy of Sciences* 2005;1066:54–66. [PubMed: 16533918]
9. Minton AP. Macromolecular crowding. *Curr Biol* 2006;16:R269–271. [PubMed: 16631567]
10. Ellis RJ. Molecular chaperones: avoiding the crowd. *Curr Biol* 1997;7:R531–533. [PubMed: 9285706]
11. Zimmerman SB, Trach SO. Estimation of macromolecule concentrations and excluded volume effects for the cytoplasm of *Escherichia coli*. *J Mol Biol* 1991;222:599–620. [PubMed: 1748995]
12. Dill KA. Dominant forces in protein folding. *Biochemistry* 1990;29:7133–7155. [PubMed: 2207096]
13. Dill KA, Shortle D. Denatured states of proteins. *Annu Rev Biochem* 1991;60:795–825. [PubMed: 1883209]
14. Zhou HX, Dill KA. Stabilization of proteins in confined spaces. *Biochemistry* 2001;40:11289–11293. [PubMed: 11560476]
15. Minton AP. Effect of a concentrated “inert” macromolecular cosolute on the stability of a globular protein with respect to denaturation by heat and by chaotropes: a statistical-thermodynamic model. *Biophys J* 2000;78:101–109. [PubMed: 10620277]
16. Minton AP. The influence of macromolecular crowding and macromolecular confinement on biochemical reactions in physiological media. *J Biol Chem* 2001;276:10577–10580. [PubMed: 11279227]
17. Zhou Y, Hall CK. Solute excluded-volume effects on the stability of globular proteins: A statistical thermodynamic theory. *Biopolymers* 1996;38:273–284.
18. Zhou HX. Protein folding and binding in confined spaces and in crowded solutions. *J Mol Recognit* 2004;17:368–375. [PubMed: 15362094]
19. Eggers DK, Valentine JS. Molecular confinement influences protein structure and enhances thermal protein stability. *Protein Sci* 2001;10:250–261. [PubMed: 11266611]
20. Flaugh SL, Lumb KJ. Effects of macromolecular crowding on the intrinsically disordered proteins c-Fos and p27(Kip1). *Biomacromolecules* 2001;2:538–540. [PubMed: 11749217]
21. Spencer DS, Xu K, Logan TM, Zhou HX. Effects of pH, salt, and macromolecular crowding on the stability of FK506-binding protein: an integrated experimental and theoretical study. *J Mol Biol* 2005;351:219–232. [PubMed: 15992823]
22. Byrne MP, Stites WE. Chemically crosslinked protein dimers: stability and denaturation effects. *Protein Sci* 1995;4:2545–2558. [PubMed: 8580845]
23. Byrne MP, Manuel RL, Lowe LG, Stites WE. Energetic contribution of side chain hydrogen bonding to the stability of staphylococcal nuclease. *Biochemistry* 1995;34:13949–13960. [PubMed: 7577991]
24. Riddles PW, Blakeley RL, Zerner B. Reassessment of Ellman's reagent. *Methods Enzymol* 1983;91:49–60. [PubMed: 6855597]
25. Schwehm JM, Stites WE. Application of automated methods for determination of protein conformational stability. *Methods Enzymol* 1998;295:150–170. [PubMed: 9750218]

26. Stites WE, Byrne MP, Aviv J, Kaplan M, Curtis PM. Instrumentation for automated determination of protein stability. *Anal Biochem* 1995;227:112–122. [PubMed: 7668369]
27. Shortle D. The expanded denatured state: an ensemble of conformations trapped in a locally encoded topological space. *Adv Protein Chem* 2002;62:1–23. [PubMed: 12418099]
28. Baldwin RL. A new perspective on unfolded proteins. *Adv Protein Chem* 2002;62:361–367. [PubMed: 12418110]
29. Bowler BE. Thermodynamics of protein denatured states. *Molecular bioSystems* 2007;3:88–99. [PubMed: 17245488]
30. McCarney ER, Kohn JE, Plaxco KW. Is there or isn't there? The case for (and against) residual structure in chemically denatured proteins. *Crit Rev Biochem Mol Biol* 2005;40:181–189. [PubMed: 16126485]
31. Ohnishi S, Shortle D. Effects of denaturants and substitutions of hydrophobic residues on backbone dynamics of denatured staphylococcal nuclease. *Protein Sci* 2003;12:1530–1537. [PubMed: 12824498]
32. Ackerman MS, Shortle D. Molecular alignment of denatured states of staphylococcal nuclease with strained polyacrylamide gels and surfactant liquid crystalline phases. *Biochemistry* 2002;41:3089–3095. [PubMed: 11863448]
33. Ackerman MS, Shortle D. Robustness of the long-range structure in denatured staphylococcal nuclease to changes in amino acid sequence. *Biochemistry* 2002;41:13791–13797. [PubMed: 12427042]
34. Shortle D, Ackerman MS. Persistence of native-like topology in a denatured protein in 8 M urea. *Science* 2001;293:487–489. [PubMed: 11463915]
35. Carra JH, Privalov PL. Thermodynamics of denaturation of staphylococcal nuclease mutants: an intermediate state in protein folding. *Faseb J* 1996;10:67–74. [PubMed: 8566550]
36. Eftink MR, Ionescu R, Ramsay GD, Wong CY, Wu JQ, Maki AH. Thermodynamics of the unfolding and spectroscopic properties of the V66W mutant of Staphylococcal nuclease and its 1–136 fragment. *Biochemistry* 1996;35:8084–8094. [PubMed: 8672513]
37. Ionescu RM, Eftink MR. Global analysis of the acid-induced and urea-induced unfolding of staphylococcal nuclease and two of its variants. *Biochemistry* 1997;36:1129–1140. [PubMed: 9033404]
38. Gittis AG, Stites WE, Lattman EE. The phase transition between a compact denatured state and a random coil state in staphylococcal nuclease is first-order. *J Mol Biol* 1993;232:718–724. [PubMed: 8355268]
39. Nishimura C, Riley R, Eastman P, Fink AL. Fluorescence energy transfer indicates similar transient and equilibrium intermediates in staphylococcal nuclease folding. *J Mol Biol* 2000;299:1133–1146. [PubMed: 10843864]
40. Seemann H, Winter R, Royer CA. Volume, expansivity and isothermal compressibility changes associated with temperature and pressure unfolding of Staphylococcal nuclease. *J Mol Biol* 2001;307:1091–1102. [PubMed: 11286558]
41. Paliwal A, Asthagiri D, Bossev DP, Paulaitis ME. Pressure denaturation of staphylococcal nuclease studied by neutron small-angle scattering and molecular simulation. *Biophys J* 2004;87:3479–3492. [PubMed: 15347583]
42. Goldenberg DP. Computational simulation of the statistical properties of unfolded proteins. *J Mol Biol* 2003;326:1615–1633. [PubMed: 12595269]
43. Pessela BC, Mateo C, Carrascosa AV, Vian A, Garcia JL, Rivas G, Alfonso C, Guisan JM, Fernandez-Lafuente R. One-step purification, covalent immobilization, and additional stabilization of a thermophilic poly-His-tagged beta-galactosidase from *Thermus* sp. strain T2 by using novel heterofunctional chelate-epoxy Sepabeads. *Biomacromolecules* 2003;4:107–113. [PubMed: 12523854]
44. BurtEAU N, Burton S, Crichton RR. Stabilisation and immobilisation of penicillin amidase. *FEBS Lett* 1989;258:185–189. [PubMed: 2689213]
45. Ahmad S, Anwar A, Saleemuddin M. Immobilization and stabilization of invertase on *Cajanus cajan* lectin support. *Bioresour Technol* 2001;79:121–127. [PubMed: 11480920]

46. Lopez-Gallego F, Montes T, Fuentes M, Alonso N, Grazu V, Betancor L, Guisan JM, Fernandez-Lafuente R. Improved stabilization of chemically aminated enzymes via multipoint covalent attachment on glyoxyl supports. *J Biotechnol* 2005;116:1–10. [PubMed: 15652425]
47. Panick G, Malessa R, Winter R, Rapp G, Frye KJ, Royer CA. Structural characterization of the pressure-denatured state and unfolding/refolding kinetics of staphylococcal nuclease by synchrotron small-angle X-ray scattering and Fourier-transform infrared spectroscopy. *J Mol Biol* 1998;275:389–402. [PubMed: 9466917]
48. Kohn JE, Millett IS, Jacob J, Zagrovic B, Dillon TM, Cingel N, Dothager RS, Seifert S, Thiyagarajan P, Sosnick TR, Hasan MZ, Pande VS, Ruczinski I, Doniach S, Plaxco KW. Random-coil behavior and the dimensions of chemically unfolded proteins. *Proc Natl Acad Sci U S A* 2004;101:12491–12496. [PubMed: 15314214]
49. Nishimura C, Uversky VN, Fink AL. Effect of salts on the stability and folding of staphylococcal nuclease. *Biochemistry* 2001;40:2113–2128. [PubMed: 11329280]
50. Flanagan JM, Kataoka M, Fujisawa T, Engelman DM. Mutations can cause large changes in the conformation of a denatured protein. *Biochemistry* 1993;32:10359–10370. [PubMed: 8399179]

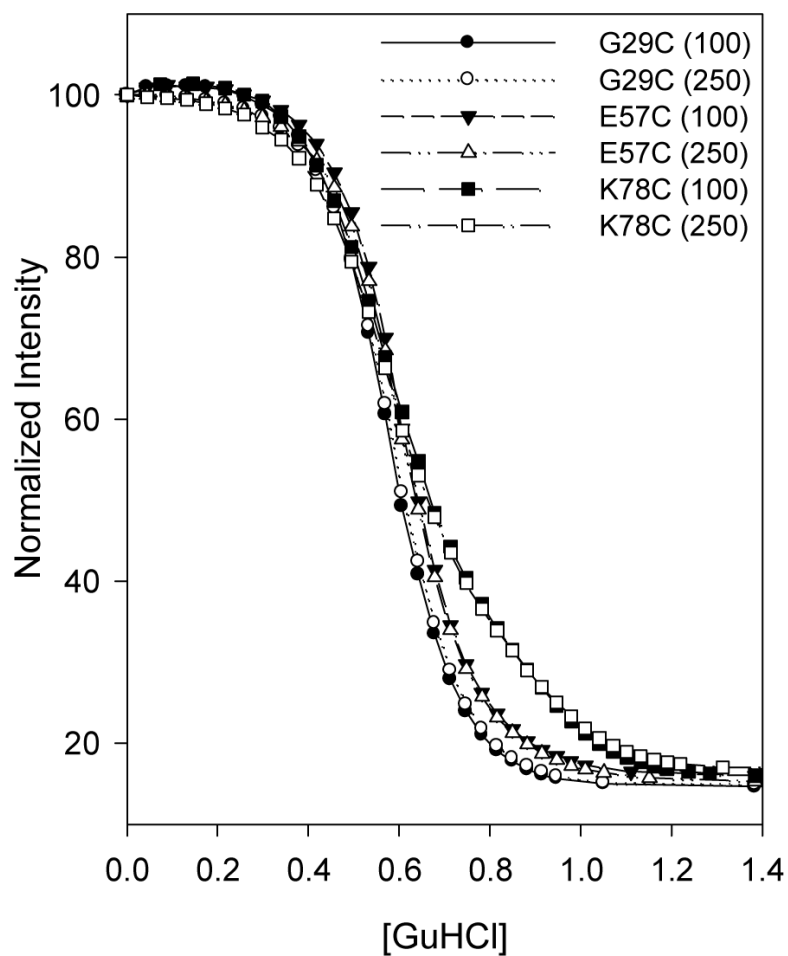
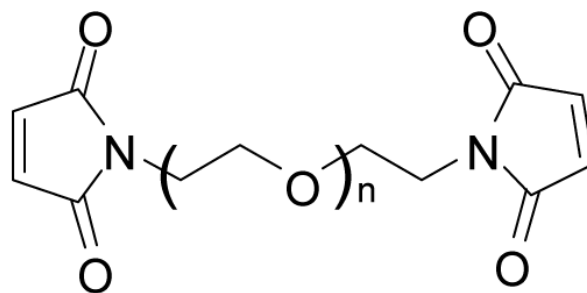
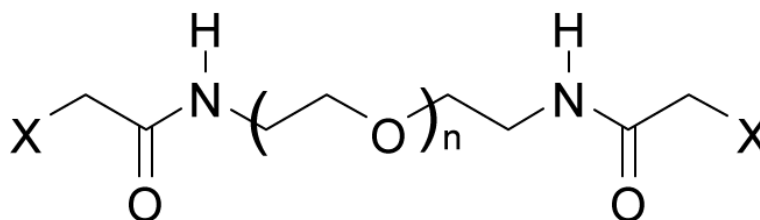


Figure 1. Normalized fluorescence intensity as a function of guanidine hydrochloride concentration for the dimers of the G29C, E57C, and K78C mutants crosslinked using bismaleimide number 2 from Figure 2. Titrations were done at starting sodium chloride concentrations of 100 and 250 nM.



1. $n = 0$
2. $n = 1$
3. $n = 2$
4. $n = 3$



5. $X = \text{Br}, n = 0$
6. $X = \text{Br}, n = 1$
7. $X = \text{Br}, n = 2$
8. $X = \text{Br}, n = 3$
9. $X = \text{I}, n = 0$
10. $X = \text{I}, n = 1$
11. $X = \text{I}, n = 2$
12. $X = \text{I}, n = 3$

Figure 2. Crosslinkers used in this study included bismaleimides 1–4, bromoacetamides 5–8, and iodoacetamides 9–12.

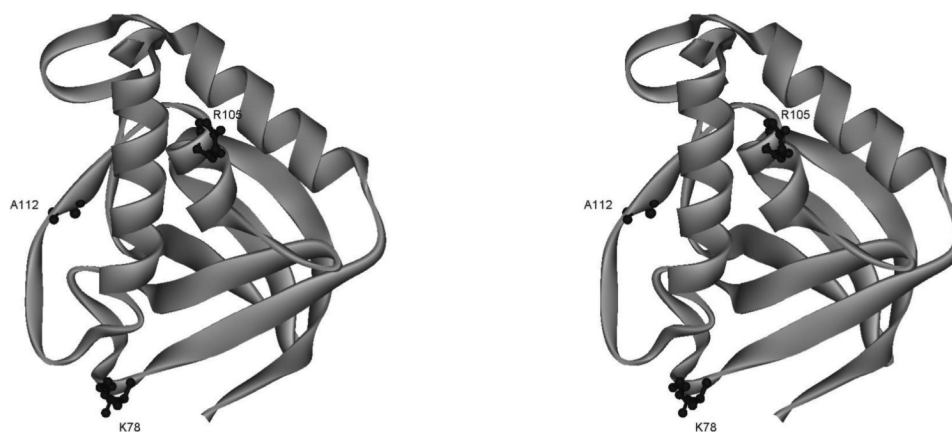


Figure 3. A stereo ribbon diagram of staphylococcal nuclease (1EY0) with the main and side chains of K78, R105, and A112 shown in ball and stick. The C-terminal helix bisects the middle of the protein in this viewing angle, with the C-terminus itself at the top of the figure.

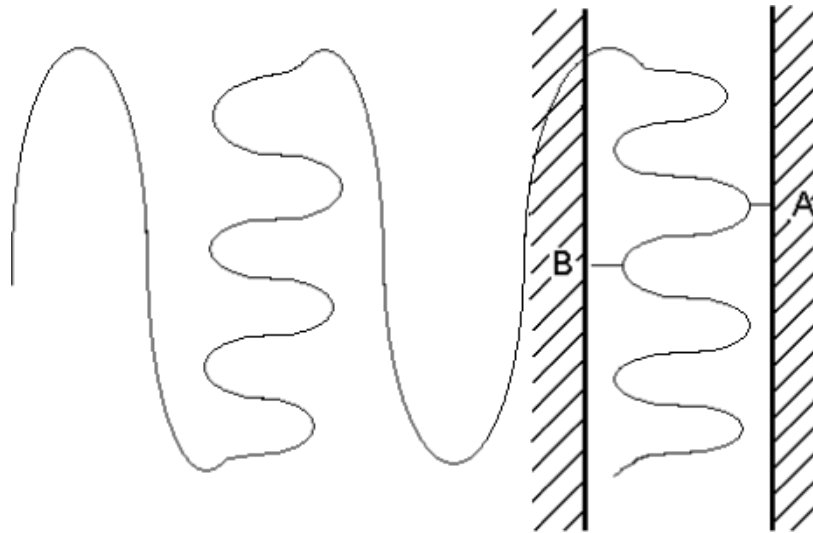


Figure 4. Representation of a hypothetical denatured state conformation. Linkage at point A is possible in this conformation but linkage at point B is not because this would require the adjacent object and the denatured protein to occupy the same space.

Stability parameters from guanidine hydrochloride denaturation of unmodified cysteine mutants and controls.

Table 1

Protein	Untreated monomers ^a		HEM treated monomers ^b		BHA treated monomers ^b	
	$\Delta G_{H_2O}^c$	C_m^d	$\Delta G_{H_2O}^c$	C_m^d	$\Delta G_{H_2O}^c$	C_m^d
G29C	4.4	0.60	4.3	0.61	4.4	0.62
G50C	4.7	0.71	4.6	0.73	4.8	0.73
E57C	4.8	0.73	4.6	0.75	4.7	0.75
A60C	4.5	0.66	4.4	0.67	4.3	0.67
K70C	4.8	0.74	4.9	0.76	4.5	0.74
K78C	5.2	0.80	5.0	0.81	4.9	0.81
R105C	2.9	0.46	2.8	0.47	2.9	0.47
A112C	4.7	0.71	4.8	0.73	4.8	0.74
K134C	4.7	0.70	4.7	0.72	4.4	0.67
WT	5.4	0.82	5.1	0.83	5.2	0.84
					$m_{G_uHCl}^e$	$m_{G_uHCl}^e$
					7.02	7.14
					6.34	6.49
					6.20	6.24
					6.50	6.42
					6.47	6.11
					6.20	6.05
					5.95	6.17
					6.49	6.48
					6.49	6.50
					6.11	6.24

^aIn 100 mM sodium chloride, 25 mM sodium phosphate, pH 7.0, 0.5 mM TCEP, 20°C. Wild-type was titrated under identical conditions except for the absence of TCEP.

^bIn 250 mM sodium chloride, 25 mM sodium phosphate, pH 7.0, 0.5 mM TCEP, 20°C. Wild-type was titrated under identical conditions except for the absence of TCEP.

^cFree energy difference between native and denatured states in the absence of denaturant in units of kcal/mol. Error estimated to be ± 0.1 kcal/mol.

^dMidpoint concentration (concentration of guanidine hydrochloride at which half of the protein molecules are denatured) in units of molar. Error estimated to be ± 0.01 M.

^eSlope value (change in free energy with respect to change in guanidine hydrochloride concentration) in units of kcal/(mol·M). Error is estimated to be ± 0.1 kcal/(mol·M).

Table 2
Denaturation parameters obtained by non-linear regression of maleimide crosslinked dimers to three state model (250 mM NaCl titrations).

Protein	Crosslinker	$\Delta G^{\ddagger}_{H_2O}$ ^a	C^{\ddagger}_m ^b	m^{\ddagger}_{GuHCl} ^c	$\Delta G^{\ddagger}_{H_2O}$ ^a	C^{\ddagger}_m ^b	m^{\ddagger}_{GuHCl} ^c
G29C	n=0	3.6	0.56	6.4	3.8	0.62	6.2
	n=1	3.5	0.56	6.2	3.9	0.61	6.4
	n=2	3.7	0.57	6.5	3.7	0.60	6.2
G50C	n=3	3.8	0.55	6.9	4.2	0.63	6.7
	n=0	2.5	0.77	3.2	4.0	0.68	5.8
	n=1	2.2	0.84	2.6	3.9	0.66	5.9
E57C	n=2	3.4	0.73	4.7	3.8	0.71	5.4
	n=3	3.7	0.69	5.4	3.8	0.71	5.4
	n=0	3.3	0.64	5.2	2.8	0.60	4.7
A60C	n=1	3.5	0.63	5.6	2.8	0.58	4.8
	n=2	3.3	0.65	5.1	3.3	0.59	5.6
	n=3	3.5	0.64	5.5	3.2	0.61	5.2
K70C	n=0	2.5	0.58	4.3	3.6	0.56	6.5
	n=1	2.4	0.57	4.2	3.7	0.54	6.8
	n=2	3.0	0.59	5.1	3.4	0.56	6.0
K78C	n=3	3.1	0.59	5.3	3.2	0.55	5.8
	n=0	2.6	0.64	4.0	4.5	0.69	6.5
	n=1	3.5	0.71	4.9	3.1	0.60	5.2
R105C	n=2	3.3	0.64	5.2	3.1	0.63	6.3
	n=3	3.8	0.67	5.7	3.8	0.68	5.6
	n=0	3.4	0.53	6.5	2.4	0.79	3.0
A112C	n=1	3.5	0.52	6.7	3.0	0.73	4.1
	n=2	3.2	0.62	5.2	2.4	0.76	3.2
	n=3	3.5	0.63	5.5	4.7	0.80	5.9
K134C	n=0	1.2	0.11	11.	0.5	0.11	4.4
	n=1	1.1	0.14	7.9	0.3	0.06	4.7
	n=2	1.5	0.16	9.2	0.6	0.19	3.1
A112C	n=3	1.6	0.19	8.3	0.6	0.17	3.6
	n=0	2.4	0.48	5.0	2.0	0.63	3.2
	n=1	3.2	0.57	5.7	2.2	0.61	3.6
K134C	n=2	3.9	0.64	6.1	3.7	0.69	5.3
	n=3	3.6	0.78	4.6	4.3	0.70	6.1
	n=0	2.6	0.55	4.7	3.9	0.70	5.6
K134C	n=1	3.5	0.63	5.5	4.3	0.73	5.9
	n=2	3.7	0.64	5.7	4.1	0.72	5.7
	n=3	3.3	0.67	4.9	3.7	0.70	5.3

^a Stability of protein to reversible denaturation in units of kcal/mol fit by non-linear regression to a three state unfolding model. Superscript 1 indicates value is for first (N-N \rightleftharpoons N-D) transition and superscript 2 indicates it is for the second (N-D \rightleftharpoons D-D) transition. The average error, as returned by the fitting program, in the former was ± 0.2 kcal \cdot mol $^{-1}$ and ± 0.5 kcal \cdot mol $^{-1}$ in the latter.

^b Midpoint concentration (concentration of guanidine hydrochloride at which half of the protein molecules are denatured) in units of molar calculated from the values of ΔG_{H_2O} and m_{GuHCl} returned by non-linear regression to a three state model. Superscript indicates if value is for first (N-N \rightleftharpoons N-D) or second (N-D \rightleftharpoons D-D) transition.

^c Slope value (change in free energy with respect to change in guanidine hydrochloride concentration) fit by non-linear regression to a three state unfolding model. Superscript indicates if value is for first (N-N \rightleftharpoons N-D) or second (N-D \rightleftharpoons D-D) transition. The average error, as returned by the fitting program, in the former was ± 0.6 kcal \cdot mol $^{-1}\cdot$ M $^{-1}$ and ± 0.5 kcal \cdot mol $^{-1}\cdot$ M $^{-1}$ in the latter.

Table 3

Parameters obtained by non-linear regression of GuHCl denaturation of haloacetamide crosslinked dimers in 250 mM NaCl, 25 mM sodium phosphate, pH 7.0 dimers to three state model.

Protein	Crosslinker	$\Delta G^{\ddagger}_{H_2O}$	C^{\ddagger}_m	m^{\ddagger}_{GuHCl}	$\Delta G^{\ddagger}_{H_2O}$	C^{\ddagger}_m	m^{\ddagger}_{GuHCl}
G29C	Br,n=0	3.3	0.59	5.6	3.4	0.58	5.8
	Br,n=1	3.4	0.55	6.2	3.6	0.60	6.0
	Br,n=2	3.5	0.55	6.4	4.0	0.62	6.5
	I, n=0	3.3	0.58	5.7	3.5	0.58	6.0
	I, n=1	3.5	0.57	6.1	3.6	0.59	6.1
	I, n=2	3.2	0.58	5.5	3.4	0.58	5.9
G50C	Br,n=0	3.3	0.80	4.1	3.8	0.70	5.4
	Br,n=1	3.4	0.60	5.7	6.0	0.71	8.4
	Br,n=2	2.8	0.65	4.3	3.5	0.60	5.8
	I, n=0	3.0	0.65	4.6	3.8	0.62	6.1
	I, n=1	3.3	0.59	5.3	3.5	0.70	7.6
	I, n=2	2.9	0.65	4.5	3.5	0.61	5.8
A60C	Br,n=0	3.4	0.62	4.2	4.0	0.62	6.5
	Br,n=1	3.8	0.78	4.9	2.5	0.57	5.1
	Br,n=2	3.6	0.66	5.5	2.5	0.61	4.1
	I, n=0	4.0	0.67	5.9	2.4	0.61	4.0
	I, n=1	3.9	0.63	6.2	1.8	0.59	3.1
	I, n=2	3.5	0.64	5.5	6.4	0.86	7.4
K70C	Br,n=0	3.3	0.66	5.0	2.2	0.69	3.2
	Br,n=1	3.3	0.66	5.0	3.2	0.60	5.3
	Br,n=2	3.9	0.62	6.3	5.3	0.88	6.0
	I, n=0	1.1	0.15	7.4	1.2	0.37	3.2
	I, n=1	3.7	0.55	6.7	4.9	0.94	5.2
	I, n=2	3.6	0.95	3.8	1.5	0.43	3.5

^aStability of protein to reversible denaturation in units of kcal/mol fit by non-linear regression to a three state unfolding model. Superscript indicates if value is for first (N \rightleftharpoons N-D) or second (N-D \rightleftharpoons D-D) transition. The average error, as returned by the fitting program, in the former was ± 0.2 kcal \cdot mol $^{-1}$ and 0.5 kcal \cdot mol $^{-1}$ in the latter.

^bMidpoint concentration (concentration of guanidine hydrochloride at which half of the protein molecules are denatured) in units of molar calculated from the values of $\Delta G^{\ddagger}_{H_2O}$ and m^{\ddagger}_{GuHCl} returned by non-linear regression to a three state unfolding model. Superscript indicates if value is for first (N-N \rightleftharpoons N-D) or second (N-D \rightleftharpoons D-D) transition.

^cSlope value (change in free energy with respect to change in guanidine hydrochloride concentration) fit by non-linear regression to a three state unfolding model. Superscript indicates if value is for first (N-N \rightleftharpoons N-D) or second (N-D \rightleftharpoons D-D) transition. The average error, as returned by the fitting program, was ± 0.5 kcal \cdot mol $^{-1}\cdot$ M $^{-1}$ for both transitions.

Table 4

Values from fit of guanidine hydrochloride denaturation of bis-maleimide crosslinked dimers in 250 mM NaCl to a two state model.

Protein	Crosslinker	ΔG_{H_2O}	C_m	m_{GdnHCl}	R^2
G29C	n=0	4.3	0	7.3	0.999
	n=1	4.3	.59	0	0.999
	n=2	4.4	.58	6	0.999
	n=3	4.4	.59	1	0.999
G50C	n=0	4.4	.59	1	0.999
	n=1	4.3	.70	2	0.994
	n=2	4.7	.71	7	0.994
	n=3	4.7	.71	3	0.999
E57C	n=0	4.0	.70	3	0.999
	n=1	4.2	.62	6	0.998
	n=2	4.4	.61	3	0.998
	n=3	4.5	.62	0	0.999
A60C	n=0	4.0	.63	8	0.999
	n=1	4.0	.57	1	0.997
	n=2	4.2	.55	5	0.995
	n=3	4.2	.57	3	0.998
K70C	n=0	4.0	.57	2	0.999
	n=1	4.9	.66	8	0.993
	n=2	4.5	.65	5	0.999
	n=3	4.9	.65	5	0.999
K78C	n=0	2.4	.67	5	0.999
	n=1	2.9	.66	9	0.968
	n=2	3.3	.64	0	0.987
	n=3	3.5	.68	0	0.998
R105C	n=0	1.1	.75	9	0.998
	n=1	1.3	.14	8	0.941
	n=2	1.1	.14	0	0.979
	n=2	1.1	0	5.4	0.

Protein	Crosslinker	ΔG_{H2O}	C_m	m_{GutICI}	R^2
A112C	n=3	1.6	.21	6	919
	n=0	2.4	.22	7.1	0.
	n=1	3.1	.57	0	952
	n=2	4.4	.60	4.2	0.
	n=3	5.7	.67	0	990
	n=0	3.2	.74	5.2	0.
K134C	n=3	4.4	.63	4	989
	n=0	4.4	.68	6.5	0.
	n=1	4.4	.69	9	998
	n=2	4.4	.69	7.6	0.
	n=3	4.4	.69	5	999
	n=0	4.4	.69	5.0	0.
			.68	8	999
			.69	6	999
			.69	4	999
			.69	6.3	0.
			.69	4	999
			.69	6.3	0.
			.69	1	999

Table 5

Values from fit of guanidine hydrochloride denaturation of bis-haloacetamide crosslinked dimers in 250 mM NaCl to a two state model.

Protein	Crosslinker	ΔG_{H2O}	C_m	m_{GuHCl}	R^2
G29C	Br,n=0	4.2	0.58	7.26	0.999
	Br,n=1	4.1	0.58	7.11	0.999
	Br,n=2	4.3	0.59	7.36	0.999
	I, n=0	4.3	0.58	7.39	0.999
	I, n=1	4.3	0.59	7.38	0.999
	I, n=2	4.2	0.58	7.29	0.999
G50C	Br,n=0	5.0	0.74	6.78	0.999
	Br,n=1	4.6	0.65	6.96	0.993
	Br,n=2	4.2	0.62	6.80	0.997
	I, n=0	4.5	0.63	7.07	0.997
	I, n=1	4.4	0.65	6.84	0.996
	I, n=2	4.2	0.62	6.89	0.998
K70C	Br,n=0	4.6	0.63	7.26	0.997
	Br,n=1	4.3	0.60	7.17	0.998
	Br,n=2	4.9	0.71	6.93	0.999
	I, n=0	4.1	0.65	6.40	0.997
	I, n=1	3.8	0.66	5.76	0.993
	I, n=2	3.9	0.74	5.21	0.997
K78C	Br,n=0	3.3	0.67	4.83	0.989
	Br,n=1	4.5	0.63	7.14	0.999
	Br,n=2	3.4	0.74	4.57	0.998
	I, n=0	1.2	0.28	4.22	0.940
	I, n=1	2.6	0.74	3.46	0.988
	I, n=2	4.6	0.70	6.51	0.999

Thermal denaturation parameters of cysteine mutants, HEM alkylated monomeric controls, and bis-maleimide crosslinked dimers.

Table 6

Protein	Untreated Standard		HEM (control)		Dimer n = 0		Dimer n = 1		Dimer n = 2		Dimer n = 3	
	T_m	ΔH_{vH}	T_m	ΔH_{vH}	T_m	ΔH_{vH}	T_m	ΔH_{vH}	T_m	ΔH_{vH}	T_m	ΔH_{vH}
G29C	48.4	81	45.9	90	44.3	93	44.9	95	44.0	99	44.5	92
G50C	50.4	77	49.3	90	47.9	103	48.7	108	48.3	100	47.9	101
E57C	52.1	77	51.2	85	48.0	96	48.2	93	47.8	94	48.0	95
A60C	49.4	74	48.8	86	46.5	101	46.5	104	45.8	98	45.5	93
K70C	50.2	75	48.4	67	43.4	105	43.4	94	43.5	108	44.3	89
K78C	53.4	83	47.6	51	45.5	77	45.0	68	45.3	61	47.1	53
R105C	41.9	58	ND	ND	ND	ND	ND	ND	ND	ND	ND	ND
A112C	50.2	77	48.4	75	45.3	111	46.3	103	47.0	88	47.9	73
K134C	50.1	77	49.1	80	46.3	94	46.6	91	46.3	93	46.4	81
WT	53.0	86	ND	ND	ND	ND	ND	ND	ND	ND	ND	ND

^a T_m Melting temperature (temperature at which half of the protein molecules are unfolded) using fluorescence as probe of structure in units of °C. Error estimated to be ± 0.3 °C.

^b ΔH_{vH} Van't Hoff enthalpy (enthalpy of denaturation estimated from the van't Hoff equation) using fluorescence as probe of structure in units of kcal/mol. Error estimated to be ± 2 kcal/mol.

Table 7

Maximal sulfur to sulfur distance in Å as determined by molecular modeling.

Crosslinker	S to S distance (Å) ^a
1, n = 0	10.5
2, n = 1	14.6
3, n = 2	17.3
4, n = 3	21.3
6, 9, n = 0	11.9
7, 10 n = 1	13.8
8, 11 n = 2	16.4

^aMaximal sulfur to sulfur distance was calculated by the Hyperchem 7 Molecular Modeling program (Hypercube Inc.) after each crosslinker was optimized in an extended conformation with all possible regio- and stereochemistries for sulfur addition considered.

Table 8

The apparent difference in protein stability between the monomeric HEM alkylated proteins and the crosslinked dimers ($\Delta\Delta G_{H_2O} = \Delta G_{H_2O}(\text{HEM}) - \Delta G_{H_2O}(\text{dimer})$). These apparent stabilities are as determined by fit to two state model.

Protein	250 mM NaCl			100 mM NaCl				
	n = 0	n = 1	n = 2	n = 3	n = 0	n = 1	n = 2	n = 3
G29C	0.0	0.0	-0.1	-0.1	0.0	0.0	-0.1	-0.2
G50C	0.2	0.3	-0.1	-0.1	-0.3	-0.2	-0.1	0.0
E57C	0.6	0.4	0.2	0.1	0.3	0.3	-0.1	-0.2
A60C	0.4	0.4	0.2	0.2	0.3	0.0	0.0	0.1
K70C	0.9	0.0	0.4	0.0	0.6	0.0	0.1	-0.1
K78C	2.6	2.1	1.7	1.5	2.5	2.0	1.6	1.4
R105C	1.7	1.5	1.7	1.2	1.6	1.3	1.6	1.3
A112C	2.4	1.7	0.4	-0.9	2.4	1.5	0.0	-1.0
K134C	1.5	0.5	0.3	0.3	1.2	0.0	0.0	0.2